

## Discovery of Diaryl Imidazolidin-2-one Derivatives, a Novel Class of Muscarinic M3 Selective Antagonists (Part 1)

Ilaria Peretto,\*<sup>†</sup> Roberto Forlani,<sup>†</sup> Claudia Fossati,<sup>†</sup> Giuseppe A. M. Giardina,<sup>†</sup> Alessandra Giardini,<sup>†</sup> Matilde Guala,<sup>†</sup> Elena La Porta,<sup>†</sup> Paola Petrillo,<sup>†</sup> Stefano Radaelli,<sup>†</sup> Luigi Radice,<sup>†</sup> Luca F. Raveglia,<sup>†</sup> Enza Santoro,<sup>†</sup> Roberta Scudellaro,<sup>†</sup> Francesca Scarpitta,<sup>†</sup> Chiara Bigogno,<sup>†</sup> Paola Misiano,<sup>†</sup> Giulio M. Dondio,<sup>†</sup> Andrea Rizzi,<sup>‡</sup> Elisabetta Armani,<sup>‡</sup> Gabriele Amari,<sup>‡</sup> Maurizio Civelli,<sup>‡</sup> Gino Villetti,<sup>‡</sup> Riccardo Patacchini,<sup>‡</sup> Marco Bergamaschi,<sup>‡</sup> Maurizio Delcanale,<sup>‡</sup> Carolina Salcedo,<sup>§</sup> Andrés G. Fernández,<sup>§</sup> and Bruno P. Imbimbo\*<sup>‡</sup>

NiKem Research, Via Zambelletti 25, 20021 Baranzate, Milan, Italy, Research and Development, Chiesi Farmaceutici S.p.A., Via Palermo 26/A, 43100 Parma, Italy, and Preclinical Research and Development, Laboratorios SALVAT, Gall 30-36, 08950-Esplugues de Llobregat, Barcelona, Spain

Received October 6, 2006

Pharmacophore-based structural identification, synthesis, and structure–activity relationships of a new class of muscarinic M3 receptor antagonists, the diaryl imidazolidin-2-one derivatives, are described. The versatility of the discovered scaffold allowed for several structural modifications that resulted in the discovery of two distinct classes of compounds, specifically a class of tertiary amine derivatives (potentially useful for the treatment of overactive bladder by oral administration) and a class of quaternary ammonium salt derivatives (potentially useful for the treatment of respiratory diseases by the inhalation route of administration). In this paper, we describe the synthesis and biological activity of tertiary amine derivatives. For these compounds, selectivity for the M3 receptor toward the M2 receptor was crucial, because the M2 receptor subtype is mainly responsible for adverse systemic side effects of currently marketed muscarinic antagonists. Compound **50** showed the highest selectivity versus M2 receptor, with binding affinity for M3 receptor  $K_i = 4.8$  nM and for M2 receptor  $K_i = 1141$  nM. Functional *in vitro* studies on selected compounds confirmed the antagonist activity toward the M3 receptor and functional selectivity toward the M2 receptor.

### Introduction

Acetylcholine (ACh) acts on muscarinic and nicotinic receptors in central and peripheral nervous systems. Five distinct but homologous gene sequences coding for muscarinic receptors (m1, m2, m3, m4, and m5) have been identified and cloned.<sup>1</sup> Muscarinic receptors are predominantly expressed in the parasympathetic nervous system and modulate the activity of an extraordinarily large number of physiological functions.<sup>2</sup> Individual muscarinic receptor subtypes are expressed in a complex, overlapping fashion in most tissues and cell types. However, studies using knockout mice have clarified the main role of each individual muscarinic receptor subtype in a number of physiological functions.<sup>3</sup> M1 receptors modulate neurotransmitter signaling in cortex and hippocampus. The M2 subtype mediates bradycardia, tremor, hypothermia, and autoinhibition in several brain regions. M3 receptors are involved in smooth muscle contractility, exocrine gland secretion, pupil dilatation, food intake, and weight gain. M4 receptors modulate dopamine activity in motor tracts and act as inhibitory autoreceptors in striatum. The role of the M5 receptors involves modulation of central dopamine function and the tone of cerebral blood vessels.

Muscarinic M3 receptor dysfunction has been noted in various pathophysiological states.<sup>4</sup>

Inflammation of the gastrointestinal tract in irritable bowel syndrome results in M3-mediated hypermotility.

Incontinence due to bladder hypercontractility has been demonstrated to be mediated through increased stimulation of M3 receptor subtype. Human bladder contains a mixed population of M2 and M3 receptors. Although M2 receptors predominate, the contractile response is mediated through M3 receptors,<sup>5,15</sup> and the role of M2 receptors is of minor importance.<sup>6</sup>

In asthma and in chronic obstructive pulmonary disease (COPD), inflammatory conditions lead to loss of inhibitory M2 muscarinic ACh autoreceptor function on parasympathetic nerves supplying the pulmonary smooth muscle, causing increased ACh release following vagal nerve stimulation. This dysfunction results in airway hyperreactivity mediated by increased stimulation of M3 receptors.<sup>7</sup>

On the other hand, it is well-known that M2 muscarinic receptors strongly regulate vagal control of heart rate and contraction;<sup>8</sup> interaction with this receptor subtype could then lead to significant adverse effects.

Even if muscarinic agonists (pilocarpine<sup>4</sup>) and antagonists (atropine,<sup>4</sup> oxybutynin<sup>9</sup>) have been known for over a century, little progress has been made in the discovery of receptor subtype selective compounds, and relatively few antimuscarinic compounds are in use in the clinic as a result of significant side effects. There is still, therefore, the need for highly selective muscarinic antagonists that can interact with distinct subtypes, thus avoiding the occurrence of adverse effects.

The aim of our study was the identification of novel M3 antagonists selective toward M2 receptors, suitable for oral treatment of M3-related dysfunctions.

### Pharmacophore Generation

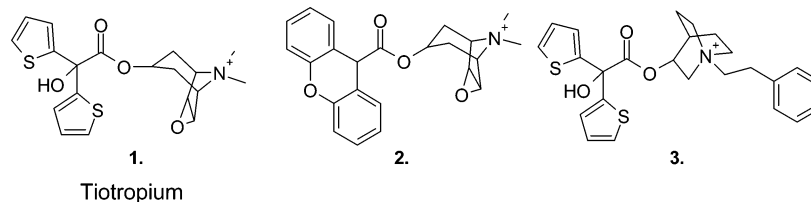
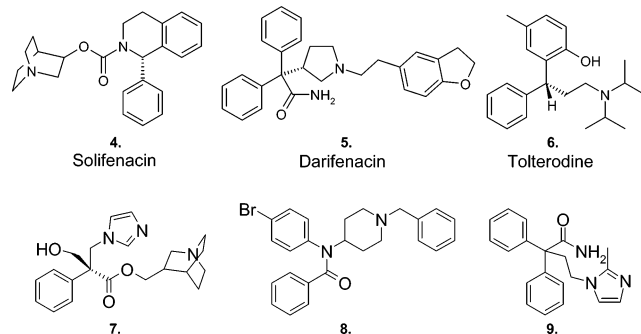
As for many other G-protein-coupled receptors, the structure of the muscarinic M3 receptor is still not known. Although several computational approaches could be pursued to identify

\* To whom correspondence should be addressed. Bruno P. Imbimbo for editorial communication and pharmacology and Ilaria Peretto for medicinal chemistry. Phone: +39 0521 279278 (B.P.I.); +39 02 356947587 (I.P.). Fax: +39 0521 279579 (B.P.I.); +39 02 356947606 (I.P.). E-mail: b.imbimbo@chiesigroup.com (B.P.I.); ilaria.peretto@nikemresearch.com (I.P.).

<sup>†</sup> NiKem Research.

<sup>‡</sup> Chiesi Farmaceutici S.p.A.

<sup>§</sup> Laboratorios SALVAT.

**Scheme 1.** Compounds in the Training Set Used to Build the M3 Pharmacophore Hypotheses**Scheme 2.** Compounds in the Validation Set Used to Prioritize the M3 Pharmacophore Hypotheses

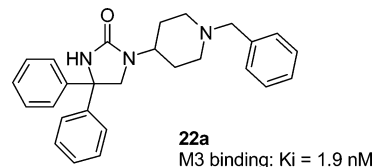
novel, potent, and selective M3 antagonists, in this case, the ligand-based design was chosen in view of the significant amount of information related to the structures of M3 receptor antagonists already available in the literature.

With the aim of defining the pharmacophoric features needed to identify M3 antagonists, a pharmacophore hypothesis was generated using Catalyst HipHop algorithm,<sup>10,11</sup> starting from the set of known muscarinic M3 receptor antagonists (training set) reported in Scheme 1. Tiotropium (compound **1**) was chosen as the reference compound in our study, because it is a recognized “gold standard” as anticholinergic agent in respiratory diseases.<sup>12</sup> Compound **2**<sup>13</sup> was chosen as a conformationally constrained analogue of tiotropium: this compound could help better define the geometric orientation of the two aromatic regions. Compound **3**<sup>14</sup> was selected as another analogue of tiotropium, in which the basic feature is differently connected to the aromatic region and differently substituted. Several common features of pharmacophore hypotheses were generated and prioritized on the basis of their ability to correctly map a validation set consisting of known muscarinic antagonists (Scheme 2).<sup>15–20</sup>

Finally, visual selection of the best pharmacophore hypothesis was performed on the basis of the best mapping of both the training and the validation compounds. The best pharmacophore hypothesis presented five features: two aromatic hydrophobic features, two hydrogen bond acceptor groups and a positive ionizable group. Pharmacophore mapping of training and validation compounds are reported in Figures 1 and 2.

The selected pharmacophore model was then utilized to search for the identified M3 antagonist key pharmacophoric features over CAP screening<sup>21</sup> and Maybridge<sup>22</sup> three-dimensional (3D) databases.<sup>23</sup> In addition, a virtual collection of compounds designed by our medicinal chemists on the basis of structural similarity with known M3 antagonists was included in the 3D searching step.

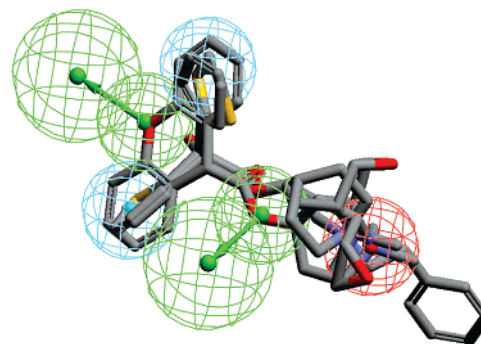
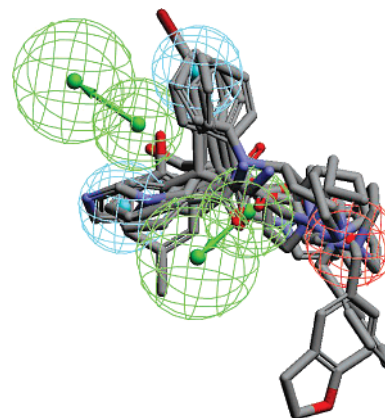
Following the usual Catalyst 3D database screening cascade and allowing virtual hits to miss one of the defined pharmacophore features, 870 commercial compounds and 58 derivatives from the virtual collection were extracted and filtered to satisfy Lipinski’s rule of five test for drug likeness and Oprea’s test for lead likeness.<sup>24,25a</sup> Furthermore, a filter to exclude molecules containing reactive groups was also included.<sup>25b</sup>

**Scheme 3.** Compound **22a** Identified as the Starting Hit Compound

The final list of compounds was prioritized in terms of fit score, conformer energy, and number of omitted features. Moreover, priority was given to noncommercial compounds to identify novel and thus patentable M3 antagonists. Considering then chemical feasibility and tractability, some of the identified compounds were selected for chemical synthesis and biological testing.

Among all the compounds tested, compound **22a** (Scheme 3) proved to be surprisingly active, despite missing one hydrogen bond acceptor feature (Figure 3); it was then selected as a starting point for further optimization.

When compound **22a** pharmacophore mapping (Figure 3) from a medicinal chemistry perspective was considered, a wide number of chemical modifications around the imidazolidine-2-

**Figure 1.** Training set compounds mapped on the selected M3 pharmacophore model. The light blue feature is an aromatic hydrophobic feature. The green feature is a hydrogen bond acceptor. The red feature is a positive ionizable group.**Figure 2.** Validation set compounds mapped on the selected M3 pharmacophore model.

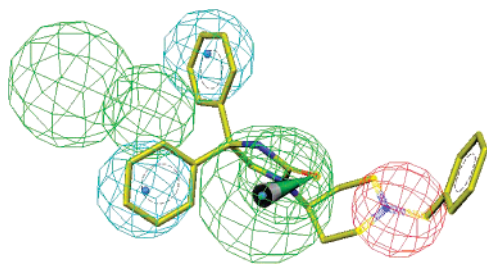


**Figure 3.** Compound **22a** (gold) matching M3 pharmacophore model.

one core could be devised (Scheme 4). The hydrophobic aromatic features suggested the possibility of substituting the aryl rings or of implementing different heterocycles (region C). The not ideal mapping of the imidazolin-2-one carbonyl group to the hydrogen bond accepting feature suggested that different substitution patterns or different heterocyclic rings should be considered (region A). Similarly, the piperidine ring can be replaced by other rings containing positive ionizable groups (region B). The benzyl moiety on the right-hand side was not included in the M3 pharmacophore model. This observation prompted the exploration of this chemical space with a chemical array of differently substituted benzyl rings and of other substituents (region D).

## Chemistry

The general synthetic pathway employed for the synthesis of most of the compounds described in this paper is reported in Scheme 5.

Hydantoin intermediates **14–18** were obtained by the Bucherer–Bergs reaction of the corresponding ketones,<sup>26</sup> performed at high temperature in a stainless steel sealed tube. Only in the case of R1 and R2 being 4-F-phenyl (hydantoin **13**), the rearrangement starting from the corresponding diketo derivative<sup>27</sup> was used because it improved the yield and made the purification easier. Hydantoin **12** was commercially available.

Hydantoin intermediates were then functionalized by Mitsunobu reaction<sup>28</sup> with hydroxyamines **20** to afford compounds of the general structure of **21a–I**. Mitsunobu reaction did not work with 4-hydroxytropine: in this case, the hydantoin moiety was functionalized by alkylation<sup>29</sup> with the mesyl derivative of general formula **19**, obtained in turn by the mesylation of 4-hydroxytropine.<sup>30</sup> Reduction of the hydantoin moiety with Red-Al (sodium bis-(2-methoxyethoxy)aluminum hydride) yielded the corresponding imidazolidin-2-one final compounds **22a–I**.

To introduce additional substituents on the amine substructure, the benzyl group was removed (debenzylation by hydrogenation),<sup>31</sup> and the basic nitrogen was further functionalized to afford compounds **24–54**, mainly by alkylation<sup>32</sup> and reductive amination,<sup>33</sup> arylation, or, in one instance, by a reaction with an acyl chloride to obtain the corresponding amide. Introduction of a methyl substituent on the imidazolidin-2-one moiety (compound **55**) was obtained by alkylation with methyl iodide.

Replacement of the imidazolidin-2-one core structure with oxazolidin-2-one (see compound **57**) required the setup of a different synthetic pathway, which is depicted in Scheme 6. Diphenyloxirane was reacted with 4-amino-*N*-benzylpiperidine to afford the amino-alcohol intermediate **56**, which was cyclized with carbonyl-diimidazole (CDI) to give the desired compound **57**.

Synthesis of 1,3,4 trisubstituted imidazolidin-2-one derivative **61** proceeded similarly, as shown in Scheme 7. Commercially available 4-phenylhydantoin failed to react both in Mitsunobu reaction conditions (with 4-hydroxy-*N*-benzylpiperidine) and by

alkylation (with 4-mesyl-*N*-benzylpiperidine); we then decided to adopt a different synthetic pathway to build the imidazolidin-2-one moiety. Amide derivative **58** was synthesized starting from *N*-Boc-protected phenylglycine by classical coupling protocol with DCC<sup>a</sup> and HOBt. Deprotection and reduction with a borane–dimethylsulfide complex afforded intermediate **59**, which was cyclized with CDI to give imidazolidin-2-one **60**. Eventually, deprotonation with sodium hydride and alkylation with benzyl bromide yielded the final compound **61**.

## Biology and ADMET

The binding affinity of the compounds toward the muscarinic M3 and M2 receptors was evaluated in membranes of CHO-K1 clone cells expressing the human M2 or M3 receptors. The nonselective muscarinic radioligand [<sup>3</sup>H]-*N*-methyl scopolamine was used to label the M2 and M3 binding sites, while the nonspecific binding was determined in the presence of cold *N*-methyl scopolamine (see Experimental Section for details and methods).

In vitro ADME developability parameters of selected compounds were explored by evaluating membrane permeability in human colon adenocarcinoma (Caco-2) cell monolayers, inhibition of major isoforms of human cytochrome P450, and hepatic microsomal clearance (see Experimental Section for details and methods).

The functional effect of this class of compounds as M3 antagonists was studied in the in vitro models of isolated mouse detrusor muscle. Functional selectivity for M3 over M2 receptors was studied in isolated rat tissues (rat detrusor muscle and left atrium).

## SAR Discussion

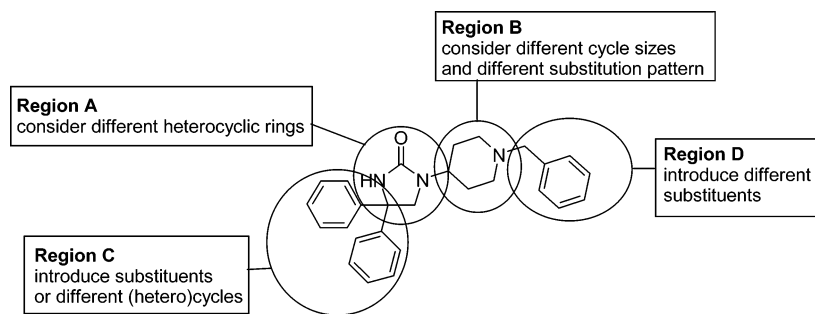
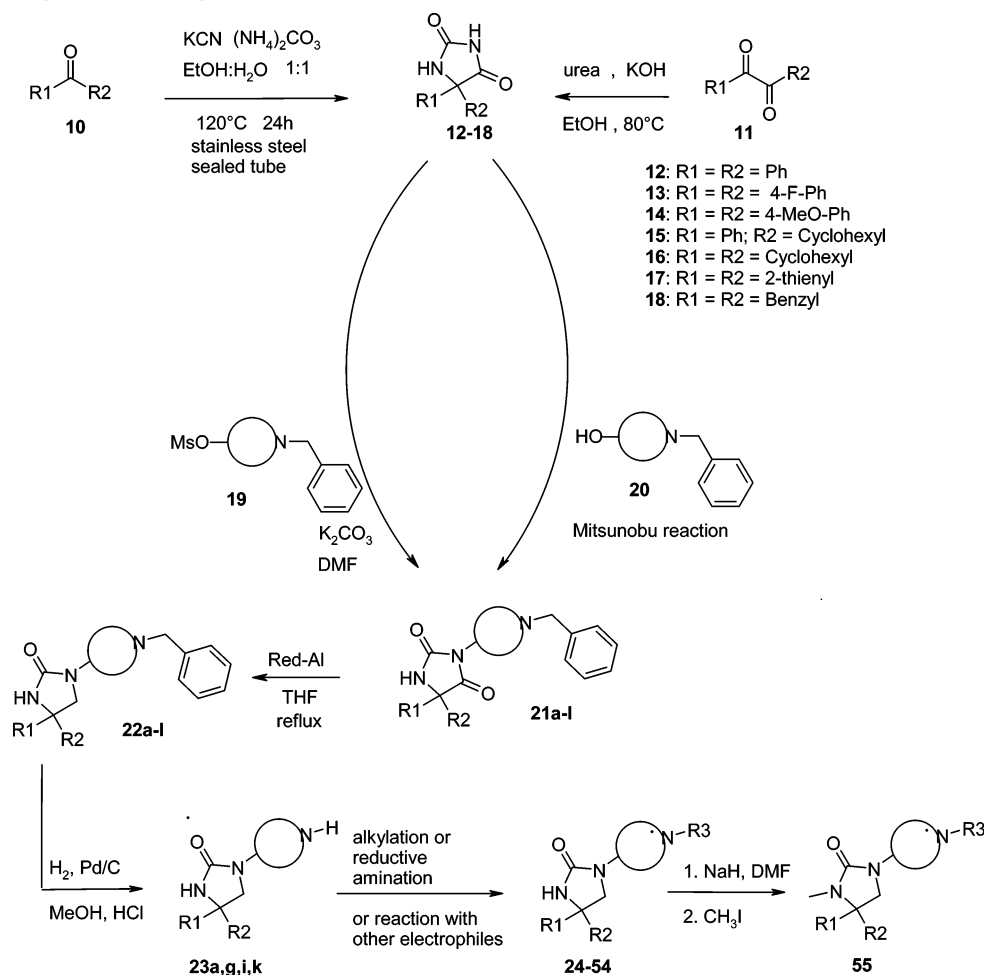
Because the starting hit **22a** was a compound endowed with a very good M3 binding affinity ( $K_i = 1.9$  nM), the main objective of the medicinal chemistry activities was to rationalize the SARs around this chemical series to improve other properties such as the selectivity toward the M2 receptor and some developability parameters. The four regions **A–D** reported in Scheme 4 were carefully investigated.

**Region A.** In Table 1, results of the investigation of the imidazolidin-2-one scaffold are reported. Whereas replacement of this scaffold with hydantoin (compound **21a**) is not tolerated, alkylation of the nitrogen at position 3 of the imidazolidin-2-one ring with a methyl group (compound **55**), or its replacement with an oxygen (compound **57**) caused a 10-fold decrease in binding affinity, without significantly affecting M2 selectivity. The good activity (although lower than for **22a**) of compounds **55** and **57** is consistent with the pharmacophoric hypothesis: in fact, no specific interactions for the NH at position 3 of the scaffold were identified.

Movement of one of the two phenyl rings of the imidazolidin-2-one scaffold onto the adjacent nitrogen (as a benzyl group, see compound **61**) also afforded a 14-fold less-active compound, with a slight reduction in M2 selectivity.

**Region B.** Replacement of the 4-piperidinyl moiety with other cyclic amines was then considered (Table 2). Shifting from 4- to 3-piperidinyl substitution (compound **22b**) proved to be detrimental for M3 affinity ( $K_i = 2.4$   $\mu$ M). Conversely, both tropine (compound **22c**) and azepine moieties (compound **22d**) allowed maintaining the same M3 binding affinity as piperidine.

<sup>a</sup> Abbreviations: DCC, dicyclohexylcarbodiimide; HOBt, 1-hydroxybenzotriazole; CDI, carbonyl-diimidazole; DCM, dichloromethane; DEAD, diethyl azodicarboxylate; DMF, *N,N*-dimethylformamide; DMSO, dimethyl sulfoxide; THF, tetrahydrofuran.

**Scheme 4.** Planned Chemical Variations on Imidazolidinone Scaffold**Scheme 5.** General Synthetic Pathway for Imidazolidinone Derivatives

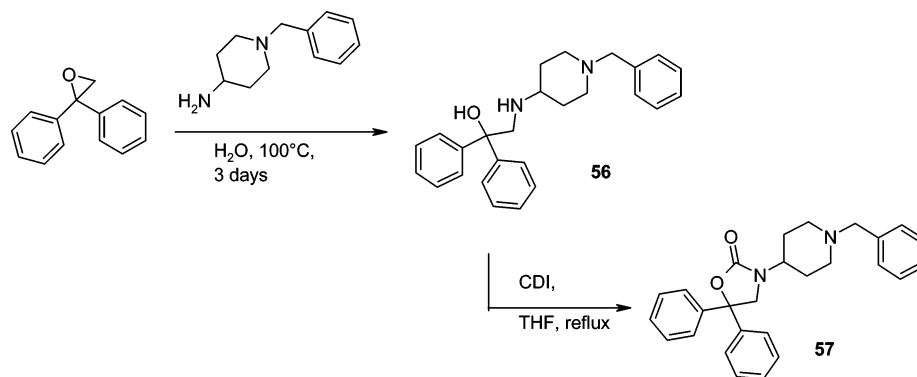
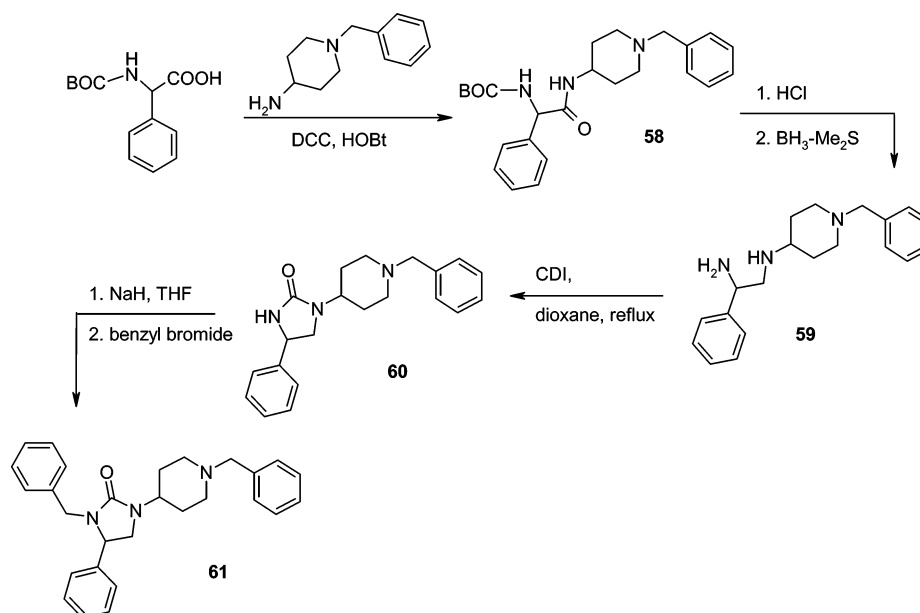
The selectivity toward M2 receptor was lost with azepine, while with tropine, some selectivity was conserved (16-fold). The (*R*)-pyrrolidine moiety (compound **22e**) proved to be slightly less active ( $K_i = 13.3$  nM) and selective (6-fold) than the hit compound **22a**, while the (*S*)-pyrrolidine derivative (compound **22f**) was almost 40-fold less active.

**Region C.** SAR exploration focused then on the investigation of the phenyl groups on the imidazolidin-2-one ring (Table 3).

Substituents at the two phenyl groups can affect both affinity and selectivity: the presence of methoxy group at the *para* position (compound **22h**) caused a significant loss of affinity ( $K_i = 114$  nM), while substitution with fluorine at the same position (compound **22g**) maintained good affinity ( $K_i = 2.8$  nM) and increased the M2 selectivity (74-fold). Replacement of one of the phenyl groups in position 4 of the imidazolidin-2-one ring with one cyclohexyl substituent (compound **22i**) did not significantly affect either the affinity or the M2 selectivity;

conversely, replacement of both of the phenyl groups with the cyclohexyl moiety (compound **22j**) caused a complete loss of activity, thus indicating that at least one aromatic moiety is necessary. Variation of the distance between the aromatic groups and the imidazolidinone core structure, as in compound **22l** featuring the dibenzyl substitution, greatly reduced the binding affinity ( $K_i = 152$  nM). Replacement of both of the phenyl groups with the 2-thienyl moiety, as in compound **22k**, preserved the same activity and selectivity profile as the hit compound **22a**.

**Region D.** The importance of the benzyl group on the basic nitrogen of the piperidine moiety was then assessed (Table 3). In fact, the inactivity of the amide derivative **24** confirmed the role of the basic nitrogen, and the low activity or inactivity of compounds **25**, **27**, and **28** proved the importance of the aromatic ring. The best distance of this ring from the basic nitrogen is one CH<sub>2</sub> unit, because shorter chains (compound **26**) or longer

**Scheme 6.** Synthesis of Oxazolidin-2-one Derivative **57****Scheme 7.** Synthesis of 1,3,4-Trisubstituted Imidazolidin-2-one Derivative **61**

chains (compounds **29**, **30** and **31**) strongly decrease the activity. Fixing this distance, we tried to replace the phenyl ring with electron poor or electron rich heteroaromatic rings (see compounds **32**, **33**, and **34**); among these, only the thienyl derivative (**33**) maintained a good activity and proved to be more selective than the parent compound ( $K_i = 13.4$  nM, 70-fold selective).

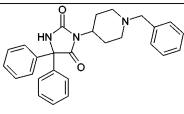
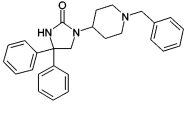
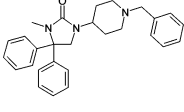
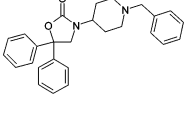
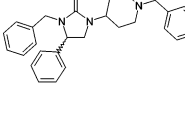
Introduction of substituents on the phenyl ring was then examined (see compounds **35**–**48**). Both electron-releasing and electron-withdrawing substituents afforded active compounds, with a marked preference for the substitution in the *meta* position, which resulted in the best combination of potency and selectivity: for example, 3-chlorobenzyl derivative **36** displayed  $K_i = 3.15$  nM and a >100-fold selectivity toward the M2 receptor. Surprisingly, disubstitution with chlorine at the *meta* position (compound **38**) afforded an inactive compound. It is worth noting that this aromatic ring, which is so important to modulate M3 activity and selectivity, was not included in the initial M3 pharmacophore. The best results obtained from the investigation of the four regions **A**–**D** were then combined to afford the mixed derivatives **49**–**54** listed in Table 3. All these compounds display good activity ( $K_i$  ranging from 1.7 nM to 6.7 nM) and good M2 selectivity (37- to 236-fold). Compounds **49** and **50** bearing the bis-(4-fluorophenyl) substitution on the imidazolidin-2-one core structure were the most selective compounds obtained in this class (143-fold and 236-fold, respectively). Compounds **53** and **54** with the bis-(2-thienyl)

moiety were less-selective (about 60-fold) but were among the most potent derivatives obtained.

The functional effect of this class of compounds as M3 antagonists was studied in the *in vitro* model of isolated mouse detrusor muscle. Increasing concentrations of carbachol (CCh) elicited strong force of contraction. In time-matched control (TMC) experiments, there was no difference between the mean  $\text{EC}_{50}$  from the first concentration–response curves (CRCs,  $1.63 \pm 0.45$   $\mu\text{M}$ ;  $n = 8$ ) and that of the second CRCs ( $\text{EC}_{50} = 1.65 \pm 0.56$   $\mu\text{M}$ ;  $n = 2$ ). The effects of compound **54** on the cumulative CRCs for CCh in mouse detrusor are summarized in Figure 4. Compound **54** deeply affected CCh-induced contractions in a concentration-dependent manner, shifting the CRCs to the right. The  $\text{pA}_2$  value calculated from Schild regression analysis for the compound was 7.9 (CI: 7.8–8.0) (slope =  $0.993 \pm 0.060$ ;  $r^2 = 0.996$ ). The corresponding  $\text{pA}_2$  value for tolterodine was 8.8 (CI: 8.5–9.0).<sup>34</sup>

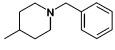
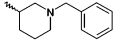
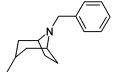
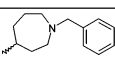
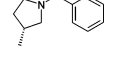
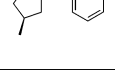
The drug effects on electric field stimulation (EFS) elicited tension in mouse detrusor are summarized in Figure 5. Force development remained stable for the duration of all the experiment. Compound **54** concentration-dependently inhibited the force of contraction, with the 1  $\mu\text{M}$  concentration producing a force reduction of  $53.72 \pm 6.45\%$  of control ( $n = 3$ ). After the wash out of the preparation, the inhibitory effects of **54** lasted for at least 2 h, suggesting a quite slow functional dissociation rate of the compound from the muscarinic receptors of the mouse detrusor muscle.

**Table 1.** Investigation of the Imidazolidin-2-one Moiety (Region A): M3 and M2 Binding Affinities

| Compound | Structure   | M3 affinity<br>(K <sub>i</sub> , nM) | M2 affinity<br>(K <sub>i</sub> , nM) | M2/M3<br>selectivity ratio |
|----------|---|--------------------------------------|--------------------------------------|----------------------------|
| 21a      |  | 2185 ± 28                            | Inactive <sup>a</sup>                |                            |
| 22a      |  | 1.9 ± 1.5                            | 80.1 ± 13.4                          | 42                         |
| 55       |  | 18.5 ± 2.3                           | 520 ± 1.1                            | 28                         |
| 57       |  | 16.8 ± 2.4                           | 908 ± 102                            | 54                         |
| 61       |  | 26.8 ± 12.9                          | 629 ± 83.6                           | 23                         |

<sup>a</sup> Inactive: Percent of control binding <50% at the concentration of 10 μM.

**Table 2.** Investigation of the Piperidine Basic Moiety (Region B): M3 and M2 Binding Affinities

| Compound | R   | M3 affinity<br>(K <sub>i</sub> , nM) | M2 affinity<br>(K <sub>i</sub> , nM) | M2/M3<br>selectivity ratio |
|----------|---|--------------------------------------|--------------------------------------|----------------------------|
| 22a      |  | 1.9 ± 1.5                            | 80.1 ± 13.4                          | 42                         |
| 22b      |  | 2445 ± 228                           | Inactive <sup>a</sup>                |                            |
| 22c      |  | 4.1 ± 1.2                            | 65 ± 22.4                            | 16                         |
| 22d      |  | 0.96 ± 0.02                          | 2.0 ± 0.8                            | 2                          |
| 22e      |  | 13.3 ± 2.6                           | 82.2 ± 4.7                           | 6                          |
| 22f      |  | 82.0 ± 15.1                          | 2272 ± 286                           | 28                         |

<sup>a</sup> Inactive: Percent of control binding <50% at the concentration of 10 μM.

The selectivity for M3 over M2 receptor was confirmed in vitro for compound **22g** in rat isolated tissues. The well-known muscarinic antagonist tolterodine was used as a reference

compound. In rat detrusor muscle (M<sub>3</sub>-mediated response), both compound **22g** and tolterodine produced a rightward parallel shift of the CRC of methacholine with pK<sub>B</sub> values of 7.77 and 8.86, respectively (Figure 6). In rat left atria (M<sub>2</sub>-mediated response), only tolterodine caused a rightward shift of the methacholine negative inotropic response in a concentration-dependent manner, with a pK<sub>B</sub> value of 8.69. Conversely, compound **22g** did not affect methacholine negative inotropic effect up to 0.1 μM.

Some of the most interesting compounds in terms of activity and selectivity were further profiled for some in vitro ADME parameters, such as inhibition of human CYP450 isoforms, intrinsic clearance (Cl<sub>i</sub>), and Caco-2 permeability as a model of intestinal absorption (Table 4). Almost all the compounds showed good permeability in the Caco-2 assay, thus indicating the possibility of good intestinal absorption. Cl<sub>i</sub> in human liver microsomes was low for all compounds; in rat microsomes, the compounds bearing the bis-(2-thienyl) moiety (**22k** and **54**) showed high Cl<sub>i</sub>, while compounds bearing the bis-(4-fluorophenyl) moiety (**22g**, **49**, and **50**) were more stable. None of the compounds tested in the CYP450 assay showed significant inhibition of any of the examined isoforms.

## Conclusions

A novel class of M3 receptor antagonists was discovered<sup>35</sup> starting from a pharmacophore model generated from known muscarinic antagonist. Study of the structure–activity relationships afforded compounds with binding affinity in the low nanomolar range, with up to >200-fold selectivity toward the M2 receptor. In vitro ADME parameters for selected derivatives indicate that this class of compounds could be suitable for systemic administration, as required for the treatment of some pathophysiological states related to M3 dysfunction, such as bladder hypercontractility. Functional in vitro studies on selected compounds confirmed the antagonist activity toward the M3 receptor and functional selectivity toward the M2 receptor. This could be an important advantage for treating overactive bladder patients.

## Experimental Section

**Computational Methodology.** In this study, chemical-feature-based pharmacophore hypotheses were generated automatically using the HipHop algorithm, as implemented in Catalyst software package (version 4.9, Accelrys, Inc., San Diego, CA) on a Silicon Graphics Fuel computer, running the IRIX 6.5 operating system.<sup>10,11</sup>

Training set and validation set compounds were edited using the Catalyst 2D/3D Visualizer, and, to generate a reasonable number of conformations able to adequately cover the molecular conformational space within a defined energy threshold, “poling” algorithm was considered to generate corresponding conformers.<sup>36</sup>

On the basis of molecular structure flexibility, the conformational analysis was carried out with the “best mode” and an optimal number of conformations equal to 200. All remaining Catalyst parameters were considered in their default settings.

Molecules and associated conformation models were submitted to Catalyst hypothesis generation.

**Pharmacophore Hypotheses Generation with HipHop.** On the basis of the chemical nature of the considered compounds, the following three features were selected to represent essential information in the hypothesis generation process: hydrogen bond acceptor (HBA), hydrophobic aromatic (HAr), and positive ionizable (PI). The objective of the HipHop run was to identify and enumerate all possible pharmacophore configurations that are in common to the training set. To perform this task, HipHop conducts an exhaustive search starting with the simplest pharmacophore configuration, that is, all possible combinations of two-feature pharmacophores. Once all two-feature pharmacophores are ex-

**Table 3.** Investigation of Substituents on the Imidazolidin-2-one (Region C) and on the Piperidine (Region D) Moieties: M3 and M2 Binding Affinities

| cmpd             | R1           | R2           | R3                        | M3 affinity<br>( $K_i$ , nM) | M2 affinity<br>( $K_i$ , nM) | M2/M3<br>selectivity<br>ratio |
|------------------|--------------|--------------|---------------------------|------------------------------|------------------------------|-------------------------------|
| 22a              | Ph           | Ph           | benzyl                    | 1.9 ± 1.5                    | 80.1 ± 13.4                  | 42                            |
| 22g              | 4-F phenyl   | 4-F phenyl   | benzyl                    | 2.8 ± 0.5                    | 207 ± 26.1                   | 74                            |
| 22h              | 4-OMe phenyl | 4-OMe phenyl | benzyl                    | 114 ± 4.0                    | inactive <sup>a</sup>        |                               |
| 22i <sup>b</sup> | phenyl       | cyclohexyl   | benzyl                    | 2.57 ± 0.47                  | 73.3 ± 18.9                  | 29                            |
| 22j              | cyclohexyl   | cyclohexyl   | benzyl                    | inactive <sup>a</sup>        |                              |                               |
| 22k              | 2-thienyl    | 2-thienyl    | benzyl                    | 2.7 ± 0.6                    | 96.8 ± 4.5                   | 36                            |
| 22l              | benzyl       | benzyl       | benzyl                    | 152 ± 63                     | 2952 ± 524                   | 19                            |
| 24               | phenyl       | phenyl       | 3-Cl benzoyl              | inactive <sup>a</sup>        |                              |                               |
| 25               | phenyl       | phenyl       | methyl                    | 923 ± 155                    | 2918 ± 280                   | 3                             |
| 26               | phenyl       | phenyl       | phenyl                    | 101 ± 22                     | inactive <sup>a</sup>        |                               |
| 27               | phenyl       | phenyl       | cyclohexyl methyl         | 354 ± 56                     | inactive <sup>a</sup>        |                               |
| 28               | phenyl       | phenyl       | propargyl                 | inactive <sup>a</sup>        |                              |                               |
| 29               | phenyl       | phenyl       | phenylethyl               | 117 ± 33                     | 411 ± 98                     | 4                             |
| 30               | phenyl       | phenyl       | phenylpropyl              | 1630 ± 116                   | 1681 ± 176                   | 1                             |
| 31               | phenyl       | phenyl       | phenoxyethyl              | 228 ± 33                     | 328 ± 63                     | 1                             |
| 32               | phenyl       | phenyl       | 3-pyridyl methyl          | 1132 ± 104                   | 302 ± 12                     | 0.3                           |
| 33               | phenyl       | phenyl       | 2-thienyl-methyl          | 13.4 ± 1.5                   | 927 ± 537                    | 69                            |
| 34               | phenyl       | phenyl       | 4-imidazolyl methyl       | 1056 ± 364                   | inactive <sup>a</sup>        |                               |
| 35               | phenyl       | phenyl       | 2-Cl benzyl               | 13.8 ± 0.4                   | inactive <sup>a</sup>        |                               |
| 36               | phenyl       | phenyl       | 3-Cl benzyl               | 3.15 ± 0.94                  | 328 ± 50.5                   | 104                           |
| 37               | phenyl       | phenyl       | 4-Cl benzyl               | 16.5 ± 0.6                   | 296 ± 74                     | 18                            |
| 38               | phenyl       | phenyl       | 3,5-Cl benzyl             | inactive <sup>a</sup>        |                              |                               |
| 39               | phenyl       | phenyl       | 2-OMe benzyl              | 83.7 ± 14.7                  | inactive <sup>a</sup>        |                               |
| 40               | phenyl       | phenyl       | 3-OMe benzyl              | 8.8 ± 1.5                    | 695 ± 55                     | 79                            |
| 41               | phenyl       | phenyl       | 4-OMe benzyl              | 25.8 ± 0.4                   | 490 ± 66                     | 19                            |
| 42               | phenyl       | phenyl       | 3-OH benzyl               | 7.6 ± 2.6                    | 47.9 ± 10.4                  | 6                             |
| 43               | phenyl       | phenyl       | 3-Me benzyl               | 2.37 ± 0.93                  | 225 ± 2.9                    | 95                            |
| 44               | phenyl       | phenyl       | 3-NH <sub>2</sub> benzyl  | 7.9 ± 0.4                    | 182 ± 12                     | 23                            |
| 45               | phenyl       | phenyl       | 3-OCF <sub>3</sub> benzyl | 2057 ± 353                   | inactive <sup>a</sup>        |                               |
| 46               | phenyl       | phenyl       | 3-CN benzyl               | 418 ± 19                     | inactive <sup>a</sup>        |                               |
| 47               | phenyl       | phenyl       | 3-CF <sub>3</sub> benzyl  | 53.5 ± 25                    | inactive <sup>a</sup>        |                               |
| 48               | phenyl       | phenyl       | 3-F benzyl                | 4.32 ± 1.42                  | 302 ± 12.5                   | 70                            |
| 49               | 4-F phenyl   | 4-F phenyl   | 3-Cl benzyl               | 6.7 ± 3.5                    | 955 ± 127                    | 143                           |
| 50               | 4-F phenyl   | 4-F phenyl   | 3-F benzyl                | 4.83 ± 2.47                  | 1141 ± 516                   | 236                           |
| 51               | phenyl       | cyclohexyl   | 3-Me benzyl               | 4.54 ± 1.76                  | 166 ± 9.4                    | 37                            |
| 52               | phenyl       | cyclohexyl   | 3-Cl benzyl               | 6.59 ± 0.38                  | 515 ± 239                    | 78                            |
| 53               | 2-thienyl    | 2-thienyl    | 3-Me benzyl               | 1.72 ± 0.39                  | 107 ± 20.6                   | 62                            |
| 54               | 2-thienyl    | 2-thienyl    | 3-F benzyl                | 2.75 ± 1.38                  | 187 ± 61                     | 68                            |

<sup>a</sup> Inactive: Percent of control binding <50% at the concentration of 10  $\mu$ M. <sup>b</sup> Racemic mixture.

hausted, it then moves to three-feature combinations. This process continues until common pharmacophore combinations can no longer be generated.<sup>23</sup> All considered training molecules were required to completely map the pharmacophore. The final HipHop output was a user-determined number of unique pharmacophores sorted from highest to lowest scoring.

**3D Database Generation.** Because the power and the efficacy of 3D database searching is dependent on both size and diversity of the compounds to be searched, we sought to extend our hit identification process beyond the limitations and bias of a commercial chemical series (CAP Screening Database<sup>21</sup> and Maybridge<sup>22</sup>) with more than 600 “in-house” designed chemical entities built on the basis of structural similarity to known muscarinic M3 antagonists. Starting from 2D structures, the 3D database of “in-house” developed compounds was obtained generating 250 conformers for each molecule with the “best” method. The overall number of conformers decreased if it provided adequate coverage for the conformational space. Accelrys supplied CAP Screening and Maybridge 3D databases in version 2002 and 2001, respectively.

**Chemistry.** <sup>1</sup>H NMR spectra were recorded on a Bruker ARX 300 (300 MHz); chemical shifts are reported downfield in parts per million (ppm) relative to TMS, utilizing the solvent peaks as

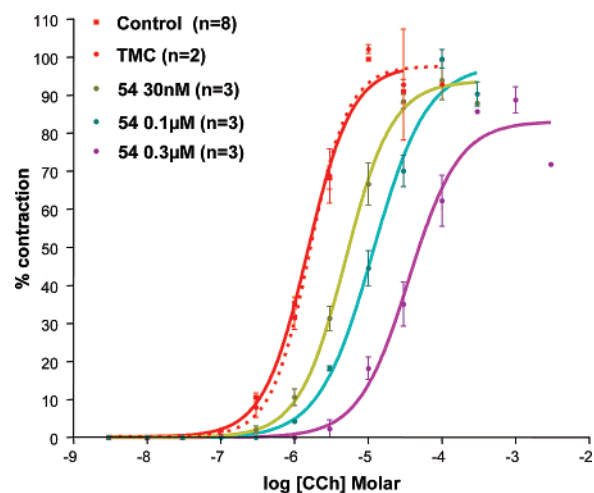


**Figure 4.** Effects of **54** on cumulative CRC for CCh in mouse detrusor strips in comparison to TMC experiments. Data are shown as means  $\pm$  SEM. Responses to CCh are expressed as percentage of the maximum effect in the first CRC. Control and TMC data are averaged values from the first CRCs in all experiments.

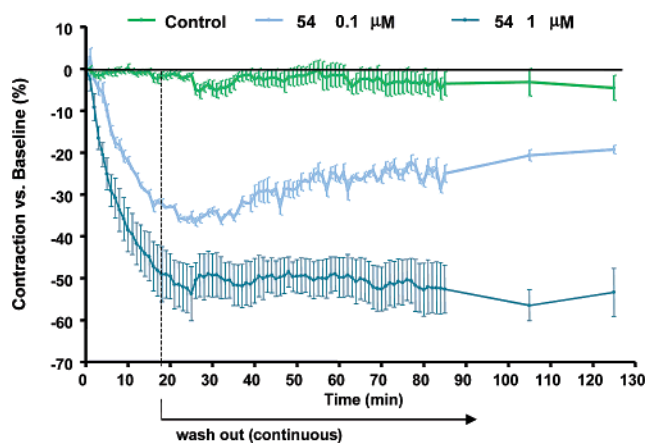


**Figure 5.** Effects of compound **54** on EFS-elicited contraction of mouse detrusor strips in comparison to experiments without any drugs added (controls). Inhibitory activity is expressed as percent reduction of the predrug control value. Data are expressed as mean values  $\pm$  SEM.

the reference. EI mass spectra were recorded on a Thermo Finnigan TSQ700 spectrometer; ESI-LCMS analysis was performed on a Phenomenex Luna C-18, 3  $\mu$ m, 4.6  $\times$  50 mm column, with an AQA Thermo Finnigan single quadrupole instrument or with a Waters Micromass ZQ2000 instrument; high performance liquid chromatography (HPLC) analysis was performed on a Shimadzu SCL-10A equipped with an SIL-10AD injector and an SPD-M10A detector normally operating in a 200–360 nm range, with a Waters Symmetry C-18, 3.5  $\mu$ m, 4.6  $\times$  75 mm column, using a 10 min gradient of 0–100% solvent B, where solvent A is 90:10:0.05 CH<sub>3</sub>CN–H<sub>2</sub>O–TFA and solvent B is 90:10:0.05 H<sub>2</sub>O–CH<sub>3</sub>CN–TFA; preparative HPLC purifications were performed on a Waters SymmetryPrep C-18, using a 20 min gradient of 0–100% solvent B, where solvent A is 99.9:0.1 H<sub>2</sub>O–TFA and solvent B is 99.9:0.1 CH<sub>3</sub>CN–TFA; reactions were monitored by TLC using 0.25 mm Merck silica gel plates (60 F254); column chromatography was performed on Merck silica gel 60 (particle size 0.063–0.2 mm); flash chromatography was conducted using a Biotage-Quad3 apparatus and prepacked silica gel columns (KP-SIL, particle size 32–60  $\mu$ m). Solid liquid extraction cartridges were purchased from Varian (“Chem Elut”, 3 mL, unbuffered, part no. 12198003). Anhydrous solvents were purchased from Aldrich and used as received. “Brine” refers to a saturated aqueous solution of NaCl. Unless otherwise specified, solutions of common inorganic salts used in workups are aqueous solutions. The <sup>1</sup>H NMR nomenclature for compounds **21a**, **22a**, **26**, **55**, **57**, and **61** refers to the structures reported in the Supporting Information.

**Synthetic Procedures. General Procedure 1. Synthesis of Hydantoin Intermediates from Ketone Derivatives. 5-Phenyl-5-cyclohexyl hydantoin (15).** Cyclohexyl phenyl ketone (0.564 g, 3 mmol) is dissolved in 20 mL of a 1:1 mixture of ethanol and water, in a stainless steel sealed tube. Potassium cyanide (0.585 g, 9 mmol) and ammonium carbonate (3.28 g, 30 mmol) are added and the mixture is heated at 120 °C for 24 h. The reaction mixture is then allowed to cool to room temperature, diluted with 20 mL of water, and cooled to 0 °C; the desired product precipitates as a white solid and is filtered to give 0.70 g of pure product. LC-MS (ESI pos): 259.37 (MH<sup>+</sup>).

Hydantoin derivatives **14**, **16**, **17**, and **18** were synthesized following the same procedure, starting from the corresponding commercially available ketones.

**Synthesis of 5,5-Di-(4-fluorophenyl) Hydantoin (13).** Bis-(4-fluorophenyl)-ethandione (1.23 g, 5 mmol) is dissolved in ethanol (20 mL); urea (0.39 g, 6.5 mmol) and potassium hydroxide (pellets, 0.476 g, 8.5 mmol) are added, and the resulting mixture is heated at 80 °C for 24 h. The reaction is allowed to cool to room temperature, diluted with water (40 mL), and cooled to 0 °C; the desired product precipitates as a white solid and is filtered to give 0.62 g of pure product. LC-MS (ESI pos): 389.22 (MH<sup>+</sup>).

**General Procedure 2. Mitsunobu Reaction. 3-(1-Benzylpiperidin-4-yl)-5,5-diphenyl-imidazolidin-2,4-dione (21a).** Commercially available 5,5-diphenyl hydantoin **12** (phenytoin, 0.50 g, 1.98 mmol) is dissolved in dry THF (20 mL); triphenyl phosphine (0.78 g, 2.97 mmol) and 4-hydroxy-*N*-benzyl piperidine (0.567 g, 2.97 mmol) are added to the reaction mixture. The resulting solution is cooled to 0 °C and diethyl azodicarboxylate (DEAD, 0.47 mL) is added dropwise. The reaction is then stirred at room temperature for 24 h. The solvent is evaporated under vacuum, and the product is purified by chromatography on silica gel (500 g, eluent: EtOAc–hexane 2:8 to EtOAc 100%), to yield 0.8 g of pure product as a white solid. LC-MS (EI pos; M<sup>+</sup>) 425.13, 334.16. <sup>1</sup>H NMR (DMSO; 343 K): 9.45 (s br, 1H, N-H), 7.53–7.32 (m, 15H, 3  $\times$  Ph), 4.25 (s br, 2H, N-CH<sub>2</sub>-Ph), 4.20 (m, 1H, N-CH-(CH<sub>2</sub>)<sub>2</sub>), 3.40 (m, 2H, H<sub>2,6</sub> eq), 3.10 (m, 2H, H<sub>2,6</sub> ax), 2.58 (m, 2H, H<sub>3,5</sub> eq), 1.87 (m, 2H, H<sub>3,5</sub> ax).

Compounds **21b**, **21d**, **21e**, **21f**, **21g**, **21h**, **21i**, **21j**, **21k**, and **21l** were synthesized following the same procedure, starting from the corresponding hydantoin derivatives.

**3-(1-Benzyl-tropin-4-yl)-5,5-diphenyl-imidazolidine-2,4-dione (21c).** (a) **Synthesis of Methanesulfonic Acid 8-Methyl-8-aza-bicyclo[3.2.1]oct-3-yl Ester (Tropine Mesilate).** *N*-Benzyl-tropin-4-ol<sup>30</sup> (0.230 g, 1.063 mmol) is added to a solution of triethyl amine (0.207 mL, 1.5 mmol) in dry DCM (10 mL); the resulting mixture is cooled to 0 °C and methanesulfonyl chloride (0.099 mL, 1.276 mmol) is added. The reaction is stirred at 0 °C for 1 h, then the solvent is evaporated under vacuum and the product obtained is employed in the next step without purification.

(b) **Synthesis of 3-(8-Methyl-8-aza-bicyclo[3.2.1]oct-3-yl)-5,5-diphenyl-imidazolidin-2,4-dione.** Commercially available 5,5-diphenyl hydantoin (phenytoin, 0.20 g, 0.793 mmol) is dissolved in dry DMF (10 mL); K<sub>2</sub>CO<sub>3</sub> (0.33 g, 2.38 mmol) and *N*-benzyl-tropine mesilate (prepared in the previous step) dissolved in dry DMF (3 mL) are added. The reaction is then stirred at 80 °C for 18 h. The reaction mixture is diluted with water and extracted with ethyl acetate; the organic phase is washed with water, then with brine, and finally dried and concentrated under vacuum to give a yellowish solid that is crystallized from ethyl ether to give the desired product as a white solid (0.18 g). LC-MS (ESI pos): 451.24 (MH<sup>+</sup>).

**General Procedure 3. Reduction with Red-Al. 3-(1-Benzylpiperidin-4-yl)-5,5-diphenyl-imidazolidin-2-one (22a).** Compound **21a** (1.0 g, 2.3 mmol) is dissolved in dry THF (20 mL) under a nitrogen atmosphere. The solution is cooled to 0 °C and a 3.5 M solution of sodium bis-(2-methoxyethoxy)aluminum hydride (Red-Al) in toluene (5.37 mL, 18.4 mmol) is added. The mixture is then heated to 85 °C for 4 h. The reaction is cooled again to 0 °C and quenched with water (5 mL); 2 M sodium hydroxide is added (10 mL), and the mixture is extracted with ethyl acetate; and the organic phase is washed with water, then with brine, and finally dried and concentrated under vacuum to give a yellowish solid that is crystallized from acetone to give the desired product as a white solid (0.80 g). LC-MS (ESI POS): 412.11 (MH<sup>+</sup>). <sup>1</sup>H NMR (CDCl<sub>3</sub> + D<sub>2</sub>O + Na<sub>2</sub>CO<sub>3</sub>): 7.37–7.15 (m, 15H, 3  $\times$  Ph), 3.94 (s, 2H, CON-CH<sub>2</sub>-C), 3.85 (m, 1H, N-CH-(CH<sub>2</sub>)<sub>2</sub>), 3.49 (s, 2H, N-CH<sub>2</sub>-Ph), 2.93 (m, 2H, H<sub>2,6</sub> eq), 2.09 (m, 2H, H<sub>2,6</sub> ax), 1.78–1.68 (m, 4H, H<sub>3,5</sub>).

Compounds **22b**, **22c**, **22d**, **22e**, **22f**, **22g**, **22h**, **22i**, **22j**, **22k**, and **22l** were synthesized following the same procedure, starting from the corresponding imidazolidin-2,4-diones.

**General Procedure 4. Hydrogenation for the Deprotection/Removal of the Benzyl Group. 5,5-Diphenyl-1-piperidin-4-yl-imidazolidin-2-one (23a).** Compound **22a** (0.50 g, 1.2 mmol) is dissolved in methanol (15 mL) and water (5 mL). Hydrochloric acid (37%, 0.5 mL) and palladium on charcoal (0.20 g) are added, and the solution is hydrogenated in a Parr apparatus (H<sub>2</sub>: 20 psi) at room temperature for 8 h. The catalyst is filtered and the clear solution is evaporated to yield the pure product as a white solid (0.380 g). LC-MS (ESI POS): 322.18 (MH<sup>+</sup>). <sup>1</sup>H NMR (CDCl<sub>3</sub> + D<sub>2</sub>O + Na<sub>2</sub>CO<sub>3</sub>): 7.37–7.21 (m, 10H), 3.94 (s, 2H), 3.91 (m, 1H),



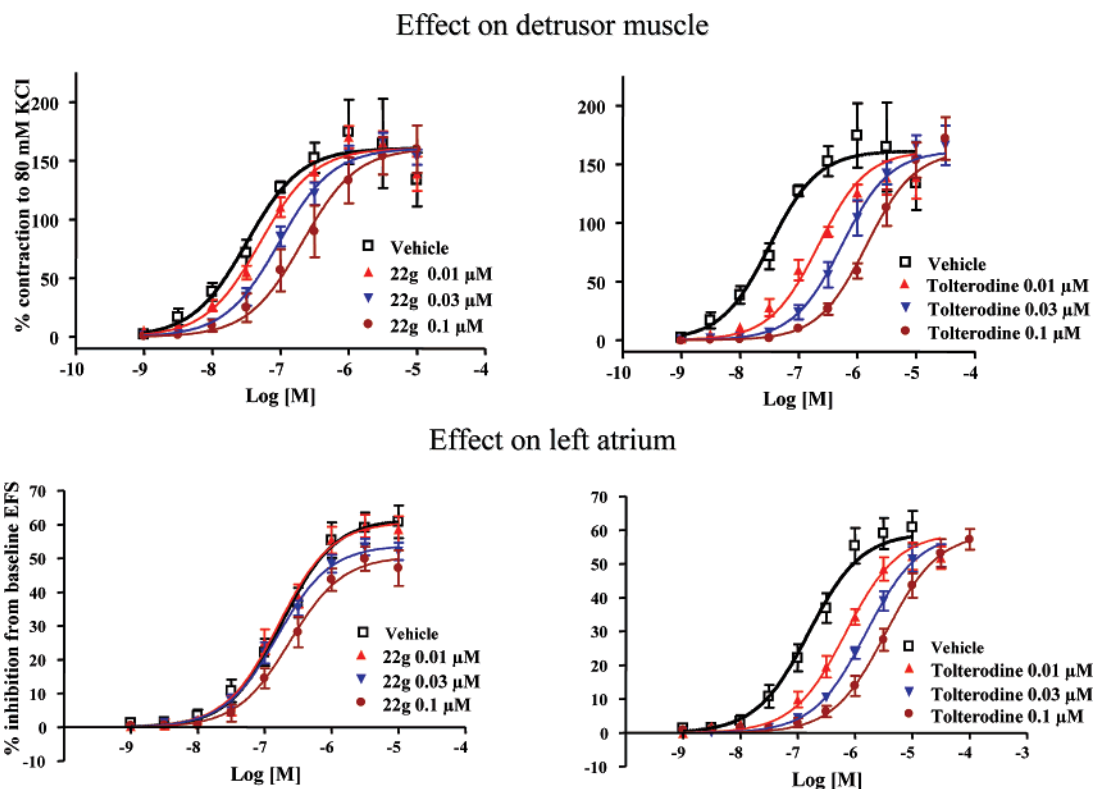


**Figure 6.** Effect of compound **22g** and tolterodine on methacholine-induced relaxation of rat detrusor muscle and rat left atrial preparations. The concentration–response relationship for methacholine either alone or in the presence of compound **22g** (0.01–0.3–0.1  $\mu\text{M}$ ) or tolterodine (0.01–0.3–0.1  $\mu\text{M}$ ) are shown. Each point represents the mean  $\pm$  SEM ( $n = 6-7$ ). Data are expressed as % of the maximal contraction induced by 80 mM KCl (for rat detrusor muscle) and as the delta % of the basal force of contraction (for rat left atrium).

**Table 4.** Evaluation of Intrinsic Clearance (Rat and Human) and P450 Profile for Some Selected Compounds

| cmpd       | M3 affinity<br>( $K_i$ , nM) | M2 affinity<br>( $K_i$ , nM) | M2/M3<br>selectivity<br>ratio | Caco-2<br>permeability | Cli (rat)<br>mL/min/g<br>liver | Cli (human)<br>mL/min/g<br>liver | CYP450<br>inhibition<br>IC <sub>50</sub> ( $\mu\text{M}$ )    |
|------------|------------------------------|------------------------------|-------------------------------|------------------------|--------------------------------|----------------------------------|---|
| <b>22a</b> | 1.9 $\pm$ 1.5                | 80.1 $\pm$ 13.4              | 42                            | high                   | 4.7                            | 1.1                              |   |
| <b>22g</b> | 2.8 $\pm$ 0.5                | 207 $\pm$ 26.1               | 74                            | high                   | 2.0                            | 0.56                             | 1A2: >100<br>2C9: 7.0<br>2C19: 12.9<br>2D6: 4.7<br>3A4: 91.9  |
| <b>22k</b> | 2.7 $\pm$ 0.6                | 96.8 $\pm$ 4.5               | 36                            | high                   | 23.7                           | 2.3                              |   |
| <b>49</b>  | 6.7 $\pm$ 3.5                | 955 $\pm$ 127                | 143                           | low                    | 1.8                            | 0.87                             | 1A2: >100<br>2C9: 4.2<br>2C19: 17.7<br>2D6: 5.3<br>3A4: >100  |
| <b>50</b>  | 4.83 $\pm$ 2.47              | 1141 $\pm$ 516               | 236                           | high                   | 1.4                            | 0.78                             | 1A2: >100<br>2C9: 7.3<br>2C19: 17.4<br>2D6: 12.0<br>3A4: >100 |
| <b>54</b>  | 2.75 $\pm$ 1.38              | 187 $\pm$ 61                 | 68                            | medium                 | 13.8                           | 0.95                             |   |

3.11 (m, 2H), 2.69 (ddd,  $J = 12.2, 2.5$  Hz, 2H), 1.76 (m, 2H), 1.58 (dq,  $J = 12.2, 4.1$  Hz, 2H).

Compounds **23g**, **23i**, and **23k** were synthesized following the same procedure, starting from the corresponding *N*-benzyl derivatives.

**General Procedure 5. Alkylation of Piperidine Derivatives.** **3-(1-(3-Chlorobenzyl)-piperidin-4-yl)-5,5-diphenyl-imidazolidin-2-one (36).** Compound **23a** (0.100 g, 0.311 mmol) is dissolved in dry DCM (10 mL), and solid  $\text{K}_2\text{CO}_3$  (0.20 g, 1.45 mmol) is added. The mixture is vigorously stirred at room temperature, and neat 3-chloro-benzyl chloride (0.051 g, 0.311 mol) is added. The reaction is stirred at room temperature for 5 h, then solid  $\text{K}_2\text{CO}_3$  is filtered, and the solution is evaporated to yield a colorless oil that is crystallized from di-isopropyl ether to afford the pure product as a

white solid (0.060 g). LC-MS (ESI pos): 446.4 ( $\text{MH}^+$ ).  $^1\text{H}$  NMR ( $\text{CDCl}_3$ ): 7.37–7.20 (m, 14H), 4.89 (s br, 1H), 3.96 (s, 2H), 3.87 (m, 1H), 3.46 (s br, 2H), 2.91 (m, 2H), 2.10 (m, 2H), 1.74 (m, 4H).

Compounds **24**, **25**, **27**, **28**, **30**, **31**, **35**, **39**, **43**, **47**, **48**, **49**, **50**, **51**, **52**, **53**, and **54** were synthesized following the same procedure, by reaction of the appropriate piperidine derivatives with the corresponding alkylating agents.

**General Procedure 6. Reductive Amination of Piperidine Derivatives.** **3-(1-(4-Chlorobenzyl)-piperidin-4-yl)-5,5-diphenyl-imidazolidin-2-one (37).** 5,5-Diphenyl-1-piperidin-4-yl-imidazolidin-2-one (compound **23a**; 0.100 g, 0.311 mmol) is dissolved in methanol (10 mL) under a nitrogen atmosphere, and 4-chlorobenzaldehyde (0.050 g, 0.341 mmol) is added. The mixture is stirred

at room temperature for 30 min, and then solid  $\text{NaBH}_3\text{CN}$  (0.040 g, 0.622 mmol) is added. The reaction is stirred at room temperature for 18 h, and then the solvent is evaporated under vacuum. The residue is dissolved in water and extracted with ethyl acetate; the organic phase is washed with water, then with brine, and finally dried and concentrated under vacuum to give a yellowish solid that is purified by flash chromatography ( $\text{SiO}_2$ , 6 g; eluent, DCM/MeOH 9:1) to give the desired product as a white solid (0.074 g). LC-MS (ESI pos): 446.4 ( $\text{MH}^+$ ).  $^1\text{H}$  NMR ( $\text{CDCl}_3 + \text{D}_2\text{O} + \text{Na}_2\text{CO}_3$ ): 7.37–7.20 (m, 14H), 3.95 (s, 2H), 3.85 (m, 1H), 3.44 (s, 2H), 2.90 (m, 2H), 2.08 (m, 2H), 1.78–1.68 (m, 4H).

Compounds **29**, **32**, **33**, **34**, **38**, **40**, **41**, **42**, **44**, **45**, and **46** were synthesized following the same procedure, by reaction of the appropriate piperidine derivatives with the corresponding aldehyde.

**3-(1-Phenyl-piperidin-4-yl)-5,5-diphenyl-imidazolidin-2-one (26)**. Compound **23a** (0.1 g, 0.3 mmol) is dissolved in DMF (1 mL). Iodobenzene (0.067 mL, 0.32 mmol), copper(I) iodide (0.061 g, 0.32 mmol), and  $\text{K}_2\text{CO}_3$  (0.045 g, 0.32 mmol) are added, and the resulting mixture is heated to 150 °C under a nitrogen atmosphere for 4 h. The mixture is then diluted with ethyl acetate and filtered over a celite pad, and the resulting solution is dried in vacuo. The product is purified by preparative HPLC to yield 45 mg of pure product as a white solid. LC-MS (ESI POS): 398.11 ( $\text{MH}^+$ ).  $^1\text{H}$  NMR ( $\text{CDCl}_3 + \text{Na}_2\text{CO}_3 + \text{D}_2\text{O}$ ): 7.39–7.19 (m, 12H,  $2 \times \text{Ph}$ ,  $H_{9,11}$ ), 6.93 (d,  $J = 8.6$  Hz, 2H,  $H_{8,12}$ ), 6.84 (dd,  $J = 7.4$ , 7.4 Hz, 1H,  $H_{10}$ ), 4.02 (m, 1H,  $H_4$ ), 3.96 (s, 2H,  $H_{14}$ ), 3.74 (m, 2H,  $H_{2,6}$  eq), 2.85 (m, 2H,  $H_{2,6}$  ax), 1.91–1.78 (m, 4H,  $H_{3,5}$ ).

**1-(1-Benzyl-piperidin-4-yl)-3-methyl-4,4-diphenyl-imidazolidin-2-one (55)**. Compound **22a** (0.100 g, 0.243 mmol) is dissolved in dry THF under nitrogen atmosphere; the solution is cooled to 0 °C and solid NaH (0.010 g, 0.243 mmol) is added. The reaction is stirred at 0 °C for 15 min, then methyl iodide (0.042 g, 0.243 mmol) is added, and the stirring is continued at room temperature for 3 h. The reaction is diluted with water and extracted with ethyl acetate; the organic phase is washed with water, then with brine, and finally dried and concentrated under vacuum to give an oil that is purified by preparative HPLC to give the desired product as a white solid (0.041 g). LC-MS (ESI pos): 426.2 ( $\text{MH}^+$ ).  $^1\text{H}$  NMR ( $\text{CDCl}_3$ , 343 K): 7.38–7.21 (m, 15H,  $3 \times \text{Ph}$ ), 3.91 (m, 1H,  $\text{N}-\text{CH}-(\text{CH}_2)_2$ ), 3.82 (s, 2H,  $\text{CON}-\text{CH}_2-\text{C}$ ), 3.55 (s br, 2H,  $\text{N}-\text{CH}_2-\text{Ph}$ ), 2.97 (m, 2H,  $H_{2,6}$  eq), 2.57 (s, 3H,  $\text{N}-\text{CH}_3$ ), 2.19 (m, 2H,  $H_{2,6}$  ax), 1.89–1.71 (m, 4H,  $H_{3,5}$ ).

**3-(1-Benzyl-piperidin-4-yl)-5,5-diphenyl-oxazolidin-2-one (57)**. **(a) 2-(1-Benzylpiperidin-4-ylamino)-1,1-diphenylethanol (56)**. A mixture of 2,2-diphenyloxirane (0.5 g, 2.55 mmol), 4-amino-*N*-benzylpiperidine (1.0 g, 5.3 mmol), and water (0.05 mL, 2.8 mmol) is heated at 100 °C for 60 h, then cooled, and passed through a silica gel pad (methylene chloride/methanol/33% aqueous ammonium hydroxide 95/5/0.5) to afford an oil (0.54 g). The crude compound was employed in the next step without purification.

**(b) 3-(1-Benzylpiperidin-4-yl)-5,5-diphenyloxazolidin-2-one (57)**. A solution of 2-(1-benzylpiperidin-4-ylamino)-1,1-diphenylethanol (**56**; 0.06 g, 0.16 mmol) and CDI (0.04 g, 0.25 mmol) in THF (3 mL) is refluxed for 24 h, cooled, and concentrated under reduced pressure. The crude material is treated with water and extracted with ethyl acetate. The organic phase is washed with brine, dried over anhydrous sodium sulfate, and concentrated under reduced pressure to afford an oil (0.07 g) that was purified by preparative HPLC, obtaining 0.03 g of pure compound. LC-MS (ESI pos): 413.1 ( $\text{MH}^+$ ).  $^1\text{H}$  NMR ( $\text{CDCl}_3 + \text{D}_2\text{O} + \text{Na}_2\text{CO}_3$ ): 7.41–7.21 (m, 15H,  $3 \times \text{Ph}$ ), 4.09 (s, 2H,  $\text{CON}-\text{CH}_2-\text{C}$ ), 3.78 (m, 1H,  $\text{N}-\text{CH}-(\text{CH}_2)_2$ ), 3.48 (s, 2H,  $\text{N}-\text{CH}_2-\text{Ph}$ ), 2.91 (m, 2H,  $H_{20,22}$  eq), 2.05 (m, 2H,  $H_{20,22}$  ax), 1.74–1.64 (m, 4H,  $H_{19,23}$ ).

**1-(1-Benzyl-piperidin-4-yl)-3-benzyl-4-phenyl-imidazolidin-2-one (61)**. **(a) 2-(*N*-tert-Butyloxycarbonyl)-amino-2-phenyl-*N*-(1-benzyl-piperidin-4-yl)-acetamide (58)**. Commercially available *N*-Boc-protected phenyl glycine (5.0 g, 19.9 mmol) is suspended in a mixture of acetonitrile (50 mL) and DCM (50 mL). The suspension is vigorously stirred under a nitrogen atmosphere. *N*-Hydroxybenzotriazole (2.97 g, 22 mmol) and DCC (4.53 g, 22 mmol) are added, and the mixture is stirred at room temperature

for 2 h. 4-Amino-*N*-benzylpiperidine (4.18 g, 22 mmol) is added, and the reaction is stirred at room temperature overnight. The reaction mixture is then diluted with DCM and washed twice with a saturated solution of potassium carbonate, water, and brine. The organic phase is dried and concentrated under vacuum to give an oil that is purified by flash chromatography ( $\text{SiO}_2$ , 120 g; eluent, DCM/MeOH 95:5) to give the desired product as a white solid (6.4 g).

**(b) *N*-2-(1-Benzylpiperidin-4-yl)-1-phenylethane-1,2-diamine Hydrochloride (59)**. 2-(*N*-tert-Butyloxycarbonyl)-amino-2-phenyl-*N*-(1-benzyl-piperidin-4-yl)-acetamide (**58**) is dissolved in DCM (80 mL) and added to a saturated solution of hydrogen chloride in diethyl ether (50 mL). The reaction mixture is stirred at room temperature for 4 h. The primary amine (dihydrochloride salt) precipitates as a white solid and is then filtered and dried under vacuum (4.5 g).

To a solution of 2-amino-*N*-(1-benzylpiperidin-4-yl)-2-phenylacetamide dihydrochloride (0.44 g, 1.15 mmol) in dry toluene (10 mL), borane–methylsulfide complex (0.22 mL, 2.3 mmol) is added under an inert atmosphere. The mixture is refluxed for 4 h, followed by the addition of MeOH (0.5 mL). After 1 h, the solution is cooled and treated with 10 mL of a 10% solution of HCl in ethyl ether. The white precipitate is filtered off and washed with ether (0.45 g).

**(c) 1-(1-Benzylpiperidin-4-yl)-4-phenyl-imidazolidin-2-one (60)**. To a suspension of *N*-2-(1-benzylpiperidin-4-yl)-1-phenylethane-1,2-diamine hydrochloride (**59**; 0.4 g, 0.95 mmol) in dry 1,4-dioxane (10 mL), CDI (0.2 g, 1.14 mmol) is added. The mixture is refluxed for 2 h, and then the solvent removed. The crude material is treated with water and extracted with ethyl acetate. The organic phase is washed with brine, dried over anhydrous sodium sulfate, and concentrated under reduced pressure to afford a white solid (0.22 g). LC-MS (ESI pos): 360.12 ( $\text{MH}^+$ ).

**(d) 1-(1-Benzyl-piperidin-4-yl)-3-benzyl-4-phenyl-imidazolidin-2-one (61)**. Compound **60** (0.100 g, 0.30 mmol) is dissolved in dry THF under a nitrogen atmosphere, the solution is cooled to 0 °C, and solid NaH (0.012 g, 0.30 mmol) is added. The reaction is stirred at 0 °C for 15 min, then benzyl bromide (0.057 g, 0.30 mmol) is added, and the stirring is continued at room temperature for 3 h. The reaction is diluted with water and extracted with ethyl acetate; the organic phase is washed with water, then with brine, and finally dried and concentrated under vacuum to give an oil that is purified by preparative HPLC to give the desired product as a white solid (0.053 g). LC-MS (ESI pos): 426.1 ( $\text{MH}^+$ ).  $^1\text{H}$  NMR ( $\text{CDCl}_3 + \text{D}_2\text{O} + \text{Na}_2\text{CO}_3$ ): 7.39–7.06 (m, 15H,  $3 \times \text{Ph}$ ), 4.89 (d,  $J = 15.1$  Hz, 1H,  $H_{25}$ ), 4.28 (dd,  $J = 8.1$ , 7.8 Hz, 1H,  $H_{15}$ ), 3.89 (m, 1H,  $H_4$ ), 3.59 (t,  $J = 8.8$  Hz, 1H,  $H_{16}$ ), 3.56 (d,  $J = 15.1$  Hz, 1H,  $H_{25}$ ), 3.49 (s, 2H,  $H_7$ ), 3.13 (dd,  $J = 8.8$ , 8.1 Hz, 1H,  $H_{15}$ ), 2.93 (m, 2H,  $H_{2,6}$  eq), 2.11 (m, 2H,  $H_{2,6}$  ax), 1.76–1.61 (m, 4H,  $H_{3,5}$ ).

**Biology and ADMET. Cell Lines and Membrane Preparations.** CHO-K1 clone cells expressing the human M2 or M3-receptors (Swissprot P08172, P20309 respectively) were harvested in  $\text{Ca}^{++}/\text{Mg}^{++}$ -free phosphate-buffered saline and collected by centrifugation at 1500 rpm for 3 min. The pellets were resuspended in ice cold buffer A (15 mM Tris-HCl pH 7.4, 2 mM  $\text{MgCl}_2$ , 0.3 mM EDTA, 1 mM EGTA) and homogenized by a PBI politron (setting 5 for 15 s). The crude membrane fraction was collected by two consecutive centrifugation steps at 40 000 *g* for 20 min at 4 °C and separated by a washing step in buffer A. The pellets obtained were finally resuspended in buffer B (75 mM Tris HCl pH 7.4, 12.5 mM  $\text{MgCl}_2$ , 0.3 mM EDTA, 1 mM EGTA, 250 mM sucrose), and aliquots were stored at –80 °C.

**Radioligand Binding Conditions.** The day of the experiment, frozen membranes were resuspended in buffer C (50 mM Tris-HCl pH 7.4, 2.5 mM  $\text{MgCl}_2$ , 1 mM EDTA). The nonselective muscarinic radioligand [ $^3\text{H}$ ]-*N*-methyl scopolamine<sup>37</sup> was used to label the M2 and M3 binding sites. Binding experiments were performed in duplicate (10-point concentration curves) in 96-well plates at a radioligand concentration of 0.1–0.3 nM. The nonspecific binding was determined in the presence of cold *N*-methyl

scopolamine (10  $\mu\text{M}$ ). Samples (final volume 0.75 mL) were incubated at room temperature for 60 min for M2 and 90 min for M3 binding assay. The reaction was terminated by a rapid filtration through GF/B Unifilter plates and two washes (0.75 mL) with cold buffer C using a Packard Filtermate Harvester. Radioactivity on the filters was measured by a microplate scintillation counter TopCount NXT (Camberra Packard).

**Membrane Permeability.** Intestinal drug absorption of test compounds was estimated in vitro using human colon adenocarcinoma (Caco-2) cell monolayers (Areta International, Gerenzano, Italy) as previously described.<sup>38</sup> Cells were suspended in DMEM and seeded ( $2 \times 10^6$  cells in 0.3 mL) in 24-well plates (Transwell, Costar, Cambridge, MA) using polycarbonate microporous cell culture inserts. Cells were grown for 21 days. The integrity of cell monolayers was checked by measuring transepithelial electrical resistance (1000  $\Omega$ ) and by the transport of the paracellular leakage marker sodium fluorescein. An amount equal to 100  $\mu\text{L}$  of test compound solution (50  $\mu\text{M}$  in 1% DMSO) was applied to the apical side. After 2 h of incubation at 37  $^\circ\text{C}$ , the apical and basolateral side solutions were removed and analyzed by liquid chromatography and tandem mass spectrometry with selected reaction monitoring. The apparent permeability ( $P_{\text{app}}$ ) was calculated as  $P_{\text{app}} = C_b V_b / (C_0 \cdot A \cdot t)$ , in which  $C_b$  = basolateral test compound concentration at time  $t$  ( $\mu\text{M}$ ),  $V_b$  = basolateral volume ( $\text{cm}^3$ ),  $C_0$  = apical test compound concentration at  $t = 0$  ( $\mu\text{M}$ ),  $A$  = filter surface area ( $\text{cm}^2$ ), and  $t$  = time (sec). The rank order of apparent permeability of the test compounds was compared with that of known reference compounds tested in the same experiment as internal standards including propranolol and cimetidine.  $P_{\text{app}}$  values were classified as “low” when  $P_{\text{app}}$  was below the limit of 10 nm/sec, “medium” when  $10 \leq P_{\text{app}} \leq 50$  nm/sec, and “high” when  $P_{\text{app}} > 50$  nm/sec.

**Inhibition of Cytochrome P450 Isoenzymes.** The assay was performed in 96-well microtiter plates according to the method described by Stresser et al.<sup>39</sup> Microsomes from baculovirus-infected insect cells (Supersomes, Gentest Corporation, Woburn, MA) expressing human cytochrome P450 isoforms (CYP1A2, CYP2C9, CYP2C19, CYP2D6, and CYP3A4) were utilized. Test compounds or standard inhibitors (dissolved in DMSO or acetonitrile) were serially diluted in a solution containing 16.3  $\mu\text{M}$  NADP<sup>+</sup>, 0.83 mM glucose-6-phosphate, 0.83 mM MgCl<sub>2</sub>, 0.4 U/mL of glucose-6-phosphate dehydrogenase, and 0.1 mg/mL microsomal protein prepared from wild-type baculovirus-infected insect cells. Appropriate control wells without inhibitor and without microsomes were also added. The plates were then pre-warmed at 37  $^\circ\text{C}$  for 10 min, and the reaction was started by adding pre-warmed enzyme/substrate mix (cytochrome P450 isoforms with their specific substrates in a 0.35 M potassium phosphate buffer at pH 7.4). Specific substrates were 3-cyano-7-ethoxycoumarin (CEC) for CYP1A2 and CYP2C19, 7-methoxy-4-trifluoromethylcoumarin (MFC) or dibenzylfluorescein (DBF) for CYP2C9, 3-[2-(*N,N*-diethyl-*N*-methylamino)ethyl]-7-methoxy-4-methylcoumarin (AMMC) for CYP2D6, and 7-benzyloxy-4-(trifluoromethyl)-coumarin (BFC) for CYP3A4. The reaction was terminated at various times, depending on the assays, by addition of a 4:1 acetonitrile/0.5 M Tris base solution. Known inhibitors for each isoenzyme (furafylline for CYP1A2, sulfaphenazole for CYP2C9, tranlycypromine for CYP2C19, quinidine for CYP2D6, and ketoconazole for CYP3A4) were tested in all assays as positive controls. Plates were read on a fluorometer (Fluoroskan Ascent, Thermo Electron Corporation, Helsinki, Finland) at the appropriate emission/excitation wavelengths. Median inhibitory concentration ( $\text{IC}_{50}$ ) was determined by nonlinear regression (GraFit software, Erithacus Software, Horley, U.K.).

**Intrinsic Clearance in Microsomes.**<sup>40</sup> Rat and human microsomes (Xenotech), at the final concentration of 0.5 mg/mL, were preincubated with test compound (0.5  $\mu\text{M}$ ) in phosphate buffer pH 7.4 for 10 min at 37  $^\circ\text{C}$ . Reaction was then started by adding the cofactor mixture solution (NADP, glucose-6-phosphate, glucose-6-phosphate dehydrogenase). Samples were taken at time 3, 6, 9, 12, 15, 18, 24, and 30 min and added to acetonitrile to stop the reaction. Samples were then centrifuged and the supernatant was

analyzed by LC-MS-MS to quantify the amount of compound. 7-Ethoxycoumarin was always tested in every experiment as the reference compound of known clearance. Data analysis: the rate constant,  $k$  ( $\text{min}^{-1}$ ), derived for the exponential decay equation is utilized to calculate the rate of Cl<sub>i</sub> of the compound using the following calculation, Cl<sub>i</sub> ( $\text{mL}/\text{min}/\text{g}$  liver) =  $k \times V \times$  microsomal protein yield, where  $V$  ( $\text{mL}/\text{mg}$  protein) = incubation volume/mg protein added and microsomal protein yield = 52.5 mg protein/g liver

**Isolated Mouse Detrusor Muscle.** CD-1 male mice (20–30 g) were killed by cervical dislocation, and the urinary bladder was isolated and placed in modified Krebs' solution (composition in mM): NaCl, 118; KCl, 4.6; CaCl<sub>2</sub>, 1.5; MgCl<sub>2</sub>, 1.5; KH<sub>2</sub>PO<sub>4</sub>, 1.15; NaHCO<sub>3</sub>, 25; and glucose, 11). Indomethacin (30  $\mu\text{M}$ ) and hexamethonium (1 mM) were included in the Krebs' solution to reduce prostaglandin-induced spontaneous activity and possible nicotinic activity, respectively. Strips of tissue ( $4 \times 2$  mm) were cut from the posterior region of bladder body, parallel to the longitudinal axis. Tissues were mounted in 25 mL organ baths containing Krebs' solution, which was maintained at 37  $^\circ\text{C}$  and constantly aerated with 95% O<sub>2</sub>/5% CO<sub>2</sub> (pH = 7.4). Isometric tension generated by the tissue was measured by pure isometric transducers (Cibertec, Spain) and recorded using the PowerLab system (ADInstruments, Australia). Tissues were maintained at a resting tension of 0.5 g during an equilibration period of 60 min. Tension adjustments were made as necessary. Tissues were washed every 15 min. The viability of each tissue was assessed by determining the contractile response to KCl (120 mM) at the start of the experimental protocol. After washing, tissues were re-equilibrated for 15 min and allowed to regain baseline tension. Repetitive CCh (3  $\mu\text{M}$ ) contractions were then induced as stimulus to obtain three consecutive contractions with less than 10% difference. After tissue equilibration, cumulative consecutive CRCs to CCh were then constructed in each bladder preparation (3 nM–30  $\mu\text{M}$ , 5 min exposure time each). The antagonist was incubated for a 60 min period between curves. The pA<sub>2</sub> was calculated for each antagonist and tissue using CCh as agonist (cumulative curve). TMC experiments were run. Peak increase in force of contraction induced by the individual CCh concentrations was expressed as percentage of the maximum effect observed during the first CRC.

In the EFS experiments, mouse strips were challenged twice with KCl (120 mM), with a 15 min washout period between exposures. After 15 min of stabilization, muscle strips were subjected to EFS. The parameter for EFS (Cibertec Stimulator CS-220, Cibertec, Spain) was pulse duration 0.3 ms at 40 Hz with 30 mA. Stimuli trains lasted 1 s at 60-s intervals. The compounds under investigation were added at fixed concentrations. Average values for the EFS-induced muscle contraction amplitudes were obtained from the last five contractions. The magnitude of drug effect is given in percent inhibition of the electrically evoked contraction amplitude before any substance addition. The functional rate of dissociation of the tested compounds from the muscarinic receptor was estimated by measuring force contraction after continuous wash out preparation (25 min after compound application). All data are expressed as the mean  $\pm$  SEM. Cumulative CRC were analyzed by nonlinear regression of each individual experiment using GraphPad Prism 4.02 (GraphPad Software Inc., San Diego, U.S.A.). Mean EC<sub>50</sub> values for CCh (molar concentration producing 50% of the maximum contraction response) were calculated for CRC before and after test drug addition. The pA<sub>2</sub> values for the antagonistic effect of test compounds on CRC for CCh were estimated from Schild plot analysis.

**Isolated Rat Detrusor Muscle and Atria.** Detrusor smooth muscle strips were excised from the bladder of female rats (250–350 g body weight) and set up in organ baths in normal Krebs–Henseleit solution at 37  $^\circ\text{C}$  under a resting tension of 1 g. Motor activity was recorded isometrically. All experiments were performed in the presence of eserine (1  $\mu\text{M}$ ). CRCs to methacholine were constructed in the absence or presence of tolterodine or compound **22g** (0.01, 0.03, and 0.1  $\mu\text{M}$ ; 60 min before, each). Contractile

responses produced by methacholine were expressed as the percent of maximal contraction produced by KCl (80 mM).

One left atrial preparation was taken from each rat, and set up occurred as described for the rat urinary bladder, under a resting tension of 0.5 g and at 33 °C. EFS was applied to preparations at a basal rate of 1 Hz, 5 ms pulse duration, and 1.5 times the threshold voltage to obtain a stabilization of contractions (basal force). Electrodes were connected to asynchronous EMKA stimulators (model STM-B01). After that, isoprenaline at 30 nM was tested, and strips having a positive inotropic response less than 10% of the basal force were discarded. CRCs to methacholine on EFS-induced twitch contractions were constructed in the absence or presence of tolterodine or compound **22g** (0.01, 0.03, and 0.1  $\mu$ M; 45 min before, each). The negative inotropic effects produced by methacholine were expressed as delta percent of the basal force of contraction. Antagonist potency of tolterodine or compound **22g** was estimated as the ability of the compounds to rightward shift CRCs to methacholine in both the rat urinary bladder and the left atrium. Competitive antagonism was checked by the Schild plot method by plotting the log of antagonist concentrations versus log-(DR-1): a plot with linear regression line and slope not significantly different from unity was considered as proof of simple reversible competition. In the Schild plot, the intercept on the abscissa (pKB) was taken as estimation of the antagonist potency.

**Acknowledgment.** This study was supported by Chiesi Farmaceutici, Parma, Italy. The authors thank Dr. Alberto Cerri, Dr. Sergio Menegon, and Dr. Samuele Pedraglio (NiKem Research) for the analytical support and Dr. Stefano Palea (Urosphere) for the functional in vitro studies on rat isolated tissues.

**Supporting Information Available:** Spectroscopic data and elemental analyses for compounds **14**, **16–18**, **21b**, **21d–I**, **22b–I**, **23g**, **23i**, **23k**, **24**, **25**, **27–35**, **38–54**. This material is available free of charge via the Internet at <http://pubs.acs.org>.

## References

- (a) Kubo, T.; Fukuda, K.; Mikami, A.; Maeda, A.; Takahashi, H.; Mishina, M.; Haga, T.; Haga, K.; Ichiyama, A.; Kanagawa, K.; Kojima, M.; Matsuo, H.; Hirose, T.; Numa, S. Cloning, sequencing and expression of complementary DNA encoding the muscarinic acetylcholine receptor. *Nature* **1986**, *323*, 441–416. (b) Eglén, R. M. Muscarinic receptor subtypes in neuronal and non-neuronal cholinergic function. *Auton. Autacoid Pharmacol.* **2006**, *26*, 219–233.
- (a) Caulfield, M. P. Muscarinic receptors—characterization, coupling and function. *Pharmacol. Ther.* **1993**, *58*, 319–379. (b) Abrams, P.; Andersson, K. E.; Buccafusco, J. J.; Chapple, C.; Chet de Groat, W.; Fryer, A. D.; Laties, A.; Nathanson, N. M.; Pasricha, P. J.; Wein, A. J. Muscarinic receptors: Their distribution and function in body systems, and the implications for treating overactive bladder. *Br. J. Pharmacol.* **2006**, *148*, 565–578.
- (a) Bymaster, F. P.; McKinzie, D. L.; Felder, C. C.; Wess, J. Use of M1–M5 muscarinic receptor knockout mice as novel tools to delineate the physiological roles of the muscarinic cholinergic system. *Neurochem. Res.* **2003**, *28*, 437–442. (b) Wess, J. Novel insights into muscarinic acetylcholine receptor function using gene targeting technology. *Trends Pharmacol. Sci.* **2003**, *24*, 414–420.
- (a) Broadley, K. J.; Kelly, D. R. Muscarinic receptor agonists and antagonists. *Molecules* **2001**, *6*, 142–193. (b) Racké, K.; Juergens, U. R.; Matthiesen, S. Control by cholinergic mechanisms. *Eur. J. Pharmacol.* **2006**, *533*, 57–68.
- Wang, P.; Luthin, G. R.; Ruggieri, M. R. Muscarinic acetylcholine receptor subtypes mediating urinary bladder contractility and coupling to GTP binding proteins. *J. Pharmacol. Exp. Ther.* **1995**, *273*, 959–966.
- Igawa, Y.; Zhang, X.; Nishizawa, O.; Umeda, M.; Iwata, A.; Taketo, M. M.; Manabe, T.; Matsui, M.; Andersson, K. E. Cystometric findings in mice lacking muscarinic M2 or M3 receptors. *J. Urol.* **2004**, *172*, 2460–2464.
- (a) Minette, P. A.; Barnes, P. J. Muscarinic receptor subtypes in lung. Clinical implications. *Am. Rev. Respir. Dis.* **1990**, *141*, S162–S165. (b) Gosens, R.; Zaagsma, J.; Meurs, H.; Halayki, A. J. Muscarinic receptor signaling in the pathophysiology of asthma and COPD. *Respir. Res.* **2006**, *7*, 73–87.
- (a) Mysliveček, J.; Trojan, S. Regulation of adrenoceptors and muscarinic receptors in the heart. *Gen. Physiol. Biophys.* **2003**, *22*, 3–14. (b) Wang, Z.; Shi, H.; Wang, H. Functional M3 muscarinic acetylcholine receptors in mammalian hearts. *Br. J. Pharmacol.* **2004**, *142*, 395–408 and references cited therein.
- Sahai, A.; Khan, M. S.; Arya, M.; John, J.; Singh, R.; Patel, H. R. The overactive bladder: Review of current pharmacotherapy in adults. Part 2: treatment options in cases refractory to anticholinergics. *Expert Opin. Pharmacother.* **2006**, *7*, 529–538.
- Catalyst*, version 4.9; Accelrys, Inc.: San Diego, CA, 2003.
- Greene, J.; Kahn, S.; Savoij, H.; Sprague, P.; Teig, S. Chemical function queries for 3D database search. *J. Chem. Inf. Comput. Sci.* **1994**, *34*, 1297–1308.
- Saberi, F.; O'Donnell, D. E. The role of tiotropium bromide, a long-acting anticholinergic bronchodilator, in the management of COPD. *Treat. Respir. Med.* **2005**, *4*, 275–281.
- Banholzer, R.; Bauer, R. New bi- and tricyclic aminoalcohol esters, their preparation and their use in medicaments. Patent DE4108393, 1991.
- Drug Data Rep.* **2001**, *23*, 550.
- Hedge, S. S. Muscarinic receptors in the bladder: From basic research to therapeutics. *Br. J. Pharmacol.* **2006**, *147*, S80–S87.
- Alabaster, V. A. Discovery and development of selective M3 antagonists for clinical use. *Life Sci.* **1997**, *60*, 1053–1060.
- Nilvebrant, L.; Hallén, B.; Larsson, G. Tolterodine—A new bladder selective muscarinic receptor antagonist: Preclinical pharmacological and clinical data. *Life Sci.* **1997**, *60*, 1129–1136.
- (a) Cross, P. E.; Stobie, A. Quinuclidine esters process and intermediate for their preparation and pharmaceutical compositions containing them. International patent WO 9306098, 1992. (b) Marriott, D. P.; Dougall, I. G.; Meghani, P.; Liu, Y.; Flower, D. F. Lead generation using pharmacophore mapping and three-dimensional database searching: Application to muscarinic M3 receptor antagonists. *J. Med. Chem.* **1999**, *42*, 3210–3216.
- Diouf, O.; Gadeau, S.; Chellé, F.; Gelbcke, M.; Talaga, P.; Christophe, B.; Gillard, M.; Massingham, R.; Guyaux, M. A new series of M3 muscarinic antagonists based on the 4-amino-piperidine scaffold. *Bioorg. Med. Chem. Lett.* **2002**, *12*, 2535–2539.
- Miyachi, H.; Kiyota, H.; Segawa, M. Novel imidazole derivatives with subtype-selective antimuscarinic activity. *Bioorg. Med. Chem. Lett.* **1998**, *8*, 2163–2168.
- CAP Screening*, Chemicals Available for Purchase Screening version; Accelrys, Inc.: San Diego, CA, 2002.
- Maybridge*, version 2001; Maybridge Chemical Company, Ltd.: Cornwall, U.K., 2001.
- (a) Kurogi, Y.; Güner, O. F. Pharmacophore modeling and three-dimensional database searching for drug design using catalyst. *Curr. Med. Chem.* **2001**, *8*, 1035–1055. (b) Hecker, E. A.; Duraiswami, C.; Andrea, T. A.; Diller, D. J. Use of catalyst pharmacophore models for screening of large combinatorial libraries. *J. Chem. Inf. Comput. Sci.* **2002**, *42*, 1204–1211.
- Lipinski, C. A.; Lombardo, F.; Dominy, B. W.; Feeney, P. J. Experimental and computational approaches to estimate solubility and permeability in drug discovery and development settings. *Adv. Drug Delivery Rev.* **1997**, *23*, 3–25.
- (a) Teague, S. J.; Davis, A. M.; Leeson, P. D.; Oprea, T. I. The design of leadlike combinatorial libraries. *Angew. Chem., Int. Ed.* **1999**, *38*, 3743–3748. (b) Excluded groups: acrylamide, acyclic diketyl, acyl halide, aldehyde, aliphatic imine, aliphatic ketone, aliphatic nitro, aliphatic (thio)ester, alkyl halide, anhydride, azide, aziridine, beta-heterosubstituted carbonyl, epoxide, halopyrimidine, hetero-allyl, iso-(thio)cyanate, maleimide, michael acceptor, perhalo ketone, phosphonate ester, phospho-, sulfonate ester, thiol, thio(urea), O–O/N–N/O–S/O–N single bonds and transition metal.
- Henze, H. R.; Furman, I. A. Researches on substituted 5-phenylidantoin. *J. Am. Chem. Soc.* **1954**, *76*, 4152–4156.
- Muccioli, G. G.; Poupaert, J. H.; Wouters, J.; Norberg, B.; Pappitz, W.; Scriba, G. K. E.; Lambert, D. M. A rapid and efficient microwave-assisted synthesis of hydantoin and thiohydantoin. *Tetrahedron* **2003**, *59*, 1301–1307.
- (a) Pelletier, J. C.; Kincaid, S. Mitsunobu reaction modifications allowing product isolation without chromatography: application to a small parallel library. *Tetrahedron Lett.* **2000**, *41*, 797–800. (b) Alcaraz, L.; Baxter, A.; Bent, J.; Bowers, K.; Braddock, M.; Clandingboel, D.; Donald, D.; Fagura, M.; Furber, M.; Laurent, C.; Lawson, M.; Mortimore, M.; McCormick, M.; Roberts, N.; Robertson, M. Novel P2X<sub>7</sub> receptor antagonists. *Bioorg. Med. Chem. Lett.* **2003**, *13*, 4043–4046.
- (a) Uscumlic, G. S.; Drmanic, S. Z.; Krstic, V. V. Reversed substituent effect on C=O stretching vibrations in hydantoin derivatives. *Indian J. Chem., Sect. B: Org. Chem. Incl. Med. Chem.* **1997**, *36*, 193–

195. (b) Kanyonyo, M.; Govaerts, S. J.; Hermans, E.; Poupaert, J. H.; Lambert, D. M. 3-Alkyl-(5,5'-diphenyl)imidazolidinediones as new cannabinoid receptor ligands. *Bioorg. Med. Chem. Lett.* **1999**, *9*, 2233–2236.
- (30) Mach, R. H.; Yang, B.; Wu, L.; Kuhner, R. J.; Whirrett, B. R.; West, T. Synthesis and sigma receptor binding affinities of 8-azabicyclo[3.2.1]octan-3a-yl and 9-azabicyclo[3.3.1]nonan-3a-yl phenyl carbamates. *Med. Chem. Res.* **2001**, *10*, 339–355.
- (31) (a) Mach, R. H.; Luedtke, R. L.; Unsworth, C. D.; Boundy, V. A.; Nowak, P. A.; Scripko, J. G.; Elder, S. T.; Jackson, J. R.; Hoffman, P. L.; Evora, P. H.; Rao, A. V.; Molinoff, P. B.; Childers, S. R.; Ehrenkauffer, R. L. <sup>18</sup>F-labeled benzamides for studying the dopamine D<sub>2</sub> receptor with positron emission tomography. *J. Med. Chem.* **1993**, *36*, 3707–3720. (b) Kiely, J. S.; Hutt, M. P.; Culbertson, T. P.; Buech, R. A.; Worth, D. F.; Lesheski, L. E.; Gogliotti, R. D.; Sennie, J. C.; Solomon, M.; Mich, T. F. Quinolone antibacterials: Preparation and activity of bridged bicyclic analogues of the C<sub>7</sub>-piperazine. *J. Med. Chem.* **1991**, *34*, 656–663.
- (32) (a) Lalinde, N.; Moliterni, J.; Wright, D.; Spencer, H. K.; Ossipov, M. H.; Spaulding, T. C.; Rudo, F. G. Synthesis and pharmacological evaluation of a series of new 3-methyl-1,4-disubstituted-piperidine analogues. *J. Med. Chem.* **1990**, *33*, 2876–2882. (b) Archibald, J. L.; Benke, G. A. Benzamidopiperidines. 2. Heterocyclic compounds related to indorammin. *J. Med. Chem.* **1974**, *17*, 736–739.
- (33) (a) Kawamoto, H.; Ozaki, S.; Itoh, Y.; Miyaji, M.; Arai, S.; Nakashima, H.; Kato, T.; Ohta, H.; Iwasawa, Y. Discovery of the first potent and selective small molecule opioid receptor-like (ORL1) antagonist: 1-[(3*R*,4*R*)-1-cyclooctylmethyl-3-hydroxymethyl-4-piperidyl]-3-ethyl-1,3-dihydro-2*H*-benzimidazol-2-one (J-113397). *J. Med. Chem.* **1999**, *42*, 5061–5063. (b) Hu, L. Y.; Ryder, T. R.; Rafferty, M. F.; Taylor, C. P.; Feng, M. R.; Kuo, B. S.; Lotarski, S. M.; Miljanich, G. P.; Millerman, E.; Siebers, K. M.; Szoke, B. G. The discovery of [1-(4-dimethylamino-benzyl)-piperidin-4-yl]-[4-(3,3-dimethylbutyl)-phenyl]-[3-methyl-but-2-enyl]-amine, an N-type Ca<sup>2+</sup> channel blocker with oral activity for analgesia. *Bioorg. Med. Chem.* **2000**, *8*, 1203–1212.
- (34) Salcedo, C.; Davalillo, S.; Catena, J.; Enrich, E.; Fernández-Serrat, A.; Miquel, I.; Sanagustín, J.; Farrerons, C.; Lagunas, C.; Balsa, D.; Fernández, A. G. Functional characterization of SVT 40776, a novel and potent M3 receptor antagonist, on mice detrusor and atria isolated preparations using in vitro and ex vivo protocols. *Br. J. Pharmacol.* **2002**, *136* (suppl), 45P.
- (35) Peretto, I.; Scarpitta, F.; La Porta, E.; Raveglia, L. F.; Giardina, G. A. M.; Imbimbo, B. P.; Rizzi, A.; Villetti, G. Preparation of imidazolone derivatives and heteroanalogues with antimuscarinic activity. International patent WO 06066924, June 29, 2006.
- (36) Smellie, A.; Teig, S. L.; Towbin, P. J. Poling: Promoting conformational variation. *J. Comp. Chem.*, **1995**, *16*, 171–187.
- (37) Haddad, E. B.; Mak, J. C.; Barnes, P. J. Characterization of [3*H*]Ba 679 BR, a slowly dissociating muscarinic antagonist, in human lung: Radioligand binding and autoradiographic mapping. *Mol. Pharmacol.* **1994**, *45*, 899–907.
- (38) Biganzoli, E.; Cavenaghi, L. A.; Rossi, R.; Brunati, M. C.; Nolli, M. L. Use of a Caco-2 cell culture model for the characterization of intestinal absorption of antibiotics. *Farmaco* **1999**, *54*, 594–599.
- (39) Stresser, D. M.; Blanchard, A. P.; Turner, S. D.; Erve, J. C.; Dandeneau, A. A.; Miller, V. P.; Crespi, C. L. Substrate-dependent modulation of CYP3A4 catalytic activity: Analysis of 27 test compounds with four fluorometric substrates. *Drug Metab. Dispos.* **2000**, *28*, 1440–1448.
- (40) Clarke, S. E.; Jeffrey, P. Utility of metabolic stability screening: Comparison of in vitro and in vivo clearance. *Xenobiotica* **2001**, *31*, 591–598.

JM061159A